Significantly Enhanced Piezocatalytic Activity of $BaTiO_3$ by Regulating the Quenching Process

Cheng-Chao Jin[a,b,#,*], Jun-Di Ai[a,#], Dai-Ming Liu[c], Li-Ning Tan[c], Liang Cao[d], Bing-Lin Shen[e], Xu-Ting Qiu[e], Ling-Xia Zhang[a,b,*]

[a] *School of Chemistry and Materials Science, Hangzhou Institute for Advanced Study, University of Chinese Academy of Sciences, 1 Sub-lane Xiangshan, Hangzhou 310024, China.*

[b] *State Key Lab of High Performance Ceramics and Superfine Microstructure, Shanghai Institute of Ceramics, Chinese Academy of Sciences, 1295 Dingxi Road, Shanghai 200050, China*

[c] *College of Electromechanical Engineering, Shandong Engineering Laboratory for Preparation and Application of High-performance Carbon-Materials, Qingdao University of Science & Technology, 99 Songling Road, Qingdao 266061, China.*

[d] *Key Laboratory of Optoelectronic Material and Device, Department of Physics, Shanghai Normal University, 100 Guilin Road, Shanghai 200234, China.*

[e] *Wuzhen Laboratory, Yangtze Delta Region Institute of Tsinghua University, 925 Daole Road, Jiaxing 314500, China..*

[#] These authors contributed equally to this work and should be considered co-first authors.

[*] Corresponding Authors: C. Jin (ccjin_cn@163.com); L. Zhang (zhlingxia@mail.sic.ac.cn).

Results

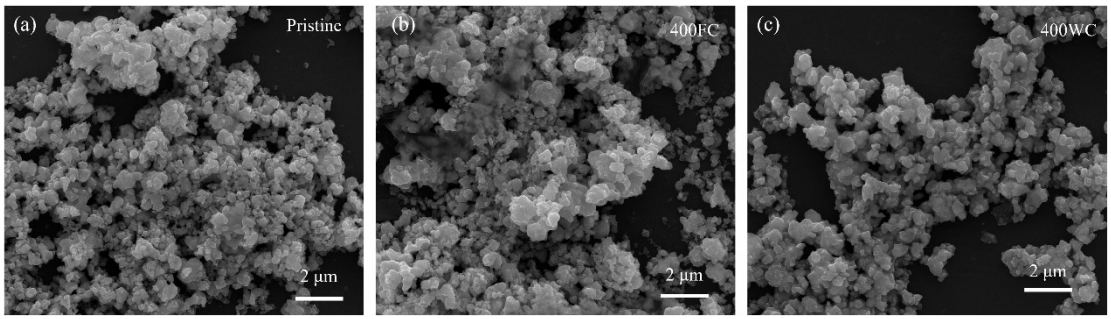

Fig. S1 SEM images of (a) the pristine BTO, (b) 400FC, and (c) 400WC

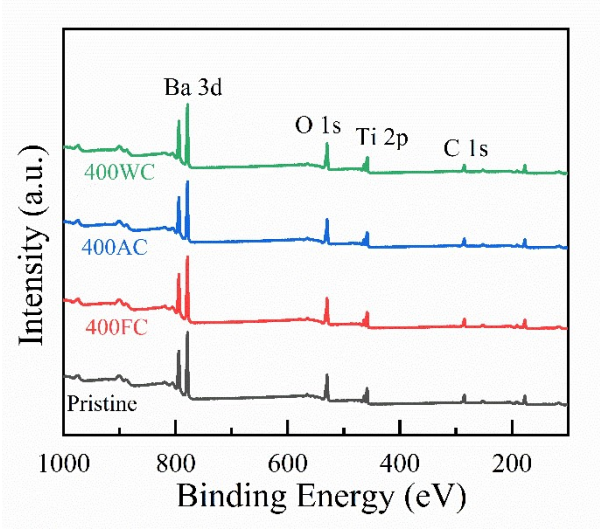

Fig. S2 XPS spectra of different BTO samples.

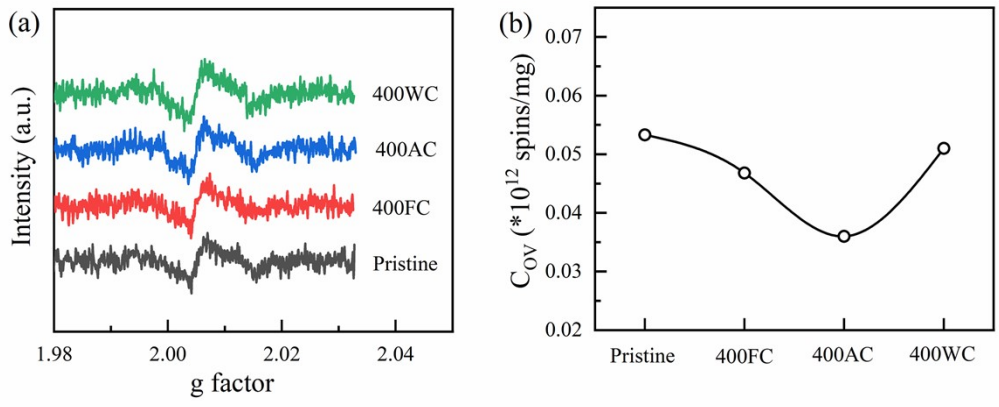

Fig. S3 (a) ESR spectra and (b) C_{OV} of different samples.

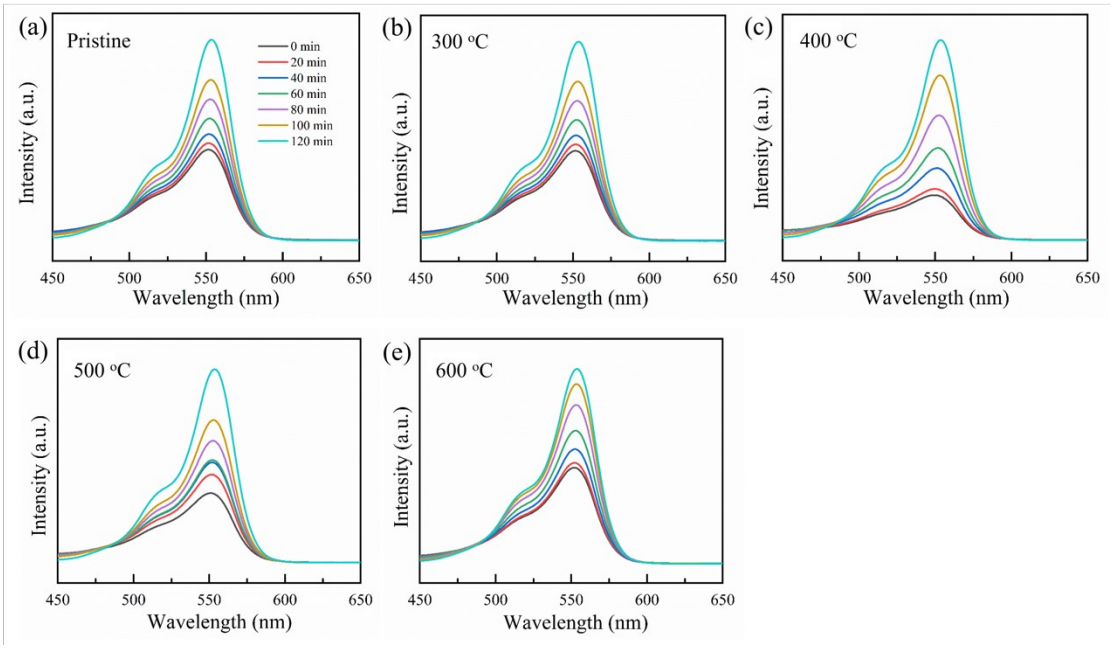

Fig. S4 UV–vis absorption spectra of RhB solution with the BTO powder calcined at different temperatures.

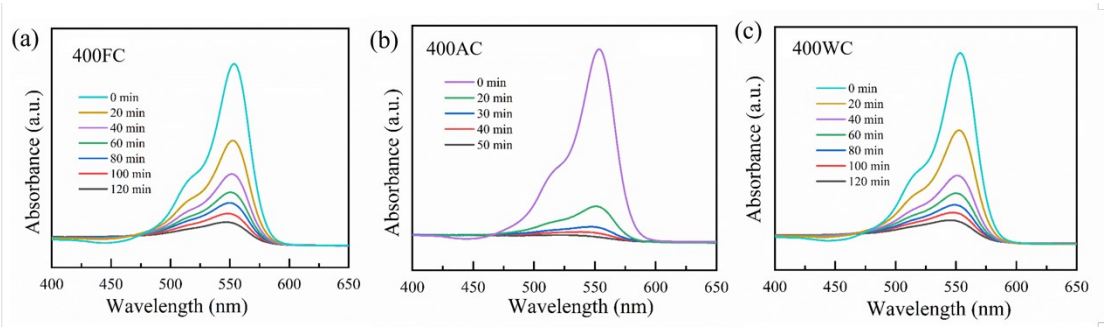

Fig. S5 UV–vis absorption spectra of RhB solution with (a) 400FC, (b) 400AC and (c) 400WC as piezocatalysts.

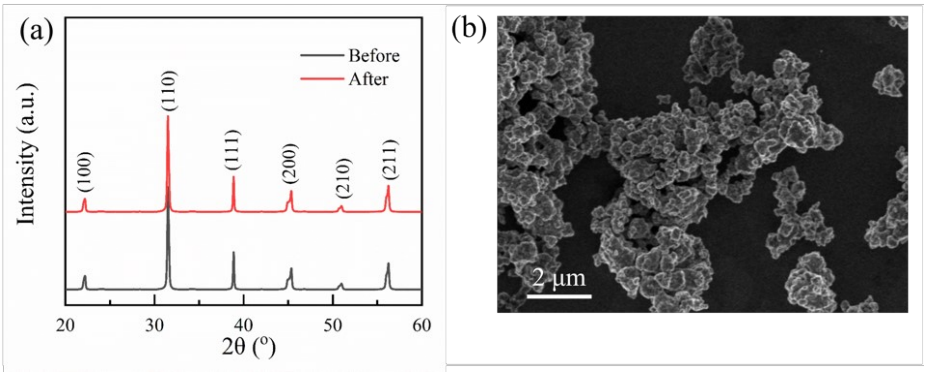

Fig. S6 XRD patterns and SEM image of 400AC after ultrasonic vibration.

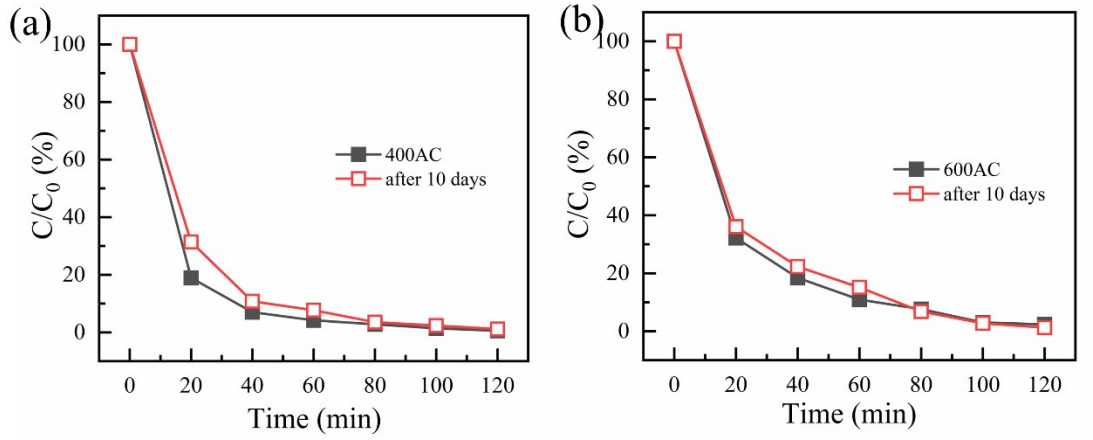

Fig. S7 Time-dependent C/C_0 of RhB degradation on (a) 400AC and (b) 600AC after being kept for 10 days.

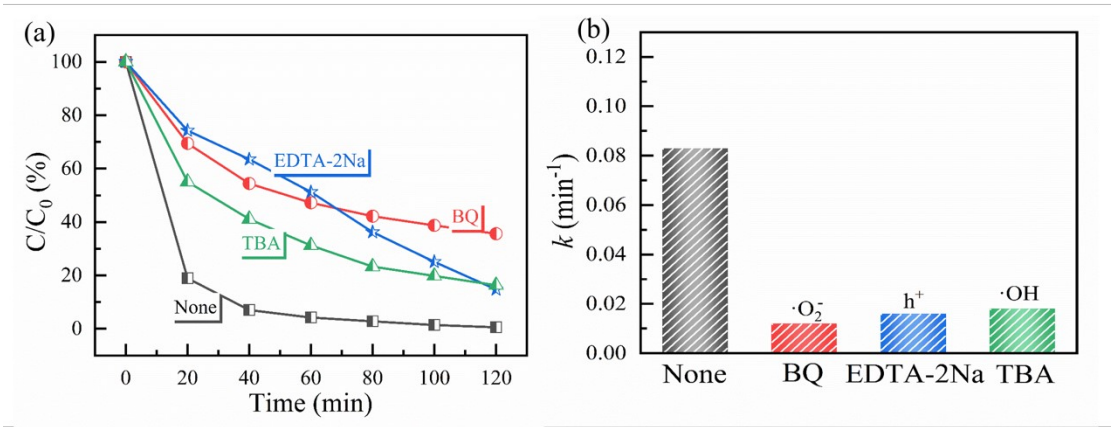

Fig. S8 (a) Time-dependent C/C_0 with the presence of scavengers and (b) the corresponding *k* values.

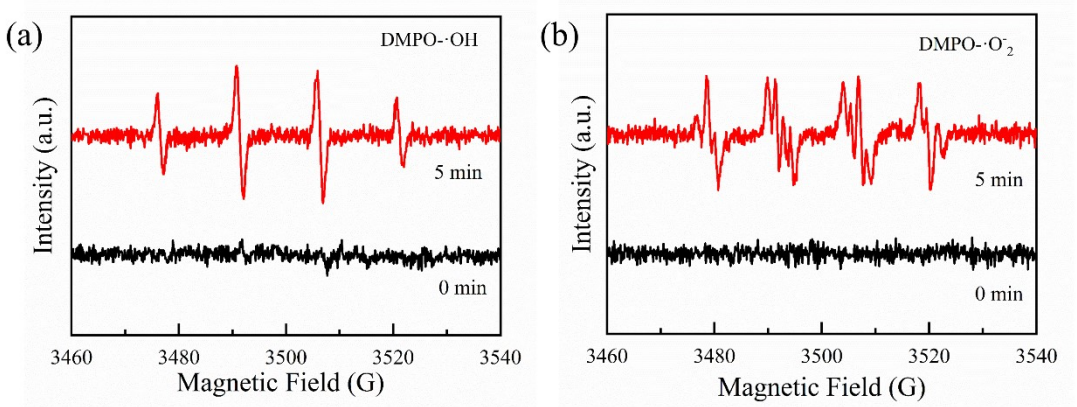

Fig. S9 ESR spectra of (a) DMPO-·OH and (b) DMPO-·O- 2 formed on 400AC.

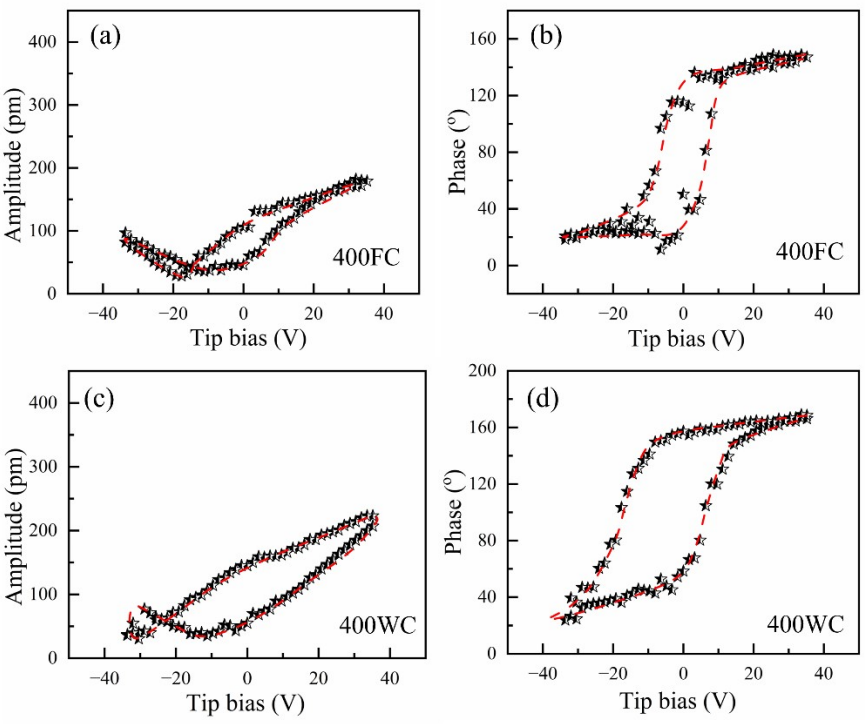

Fig. S10 PFM results: (a, c) amplitude butterfly loops and (b, d) phase hysteresis loops of (a, b) 400FC and (c, d) 400WC.

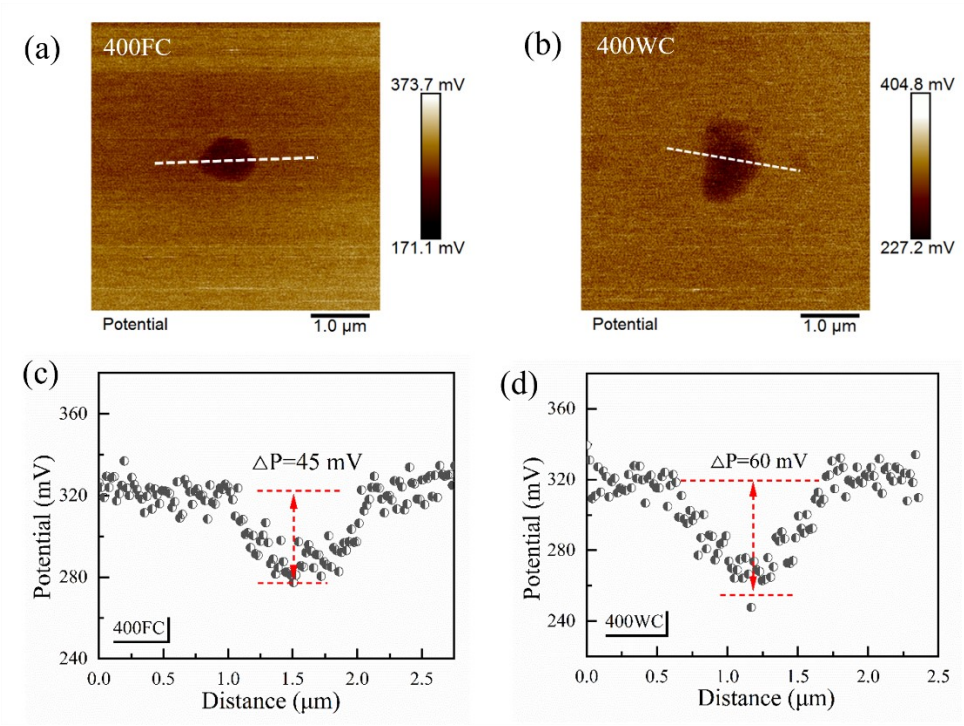

Fig. S11 (a, b) KPFM potential map and (c, d) amplitude loop of (a, c) 400FC and (b, d) 400WC.

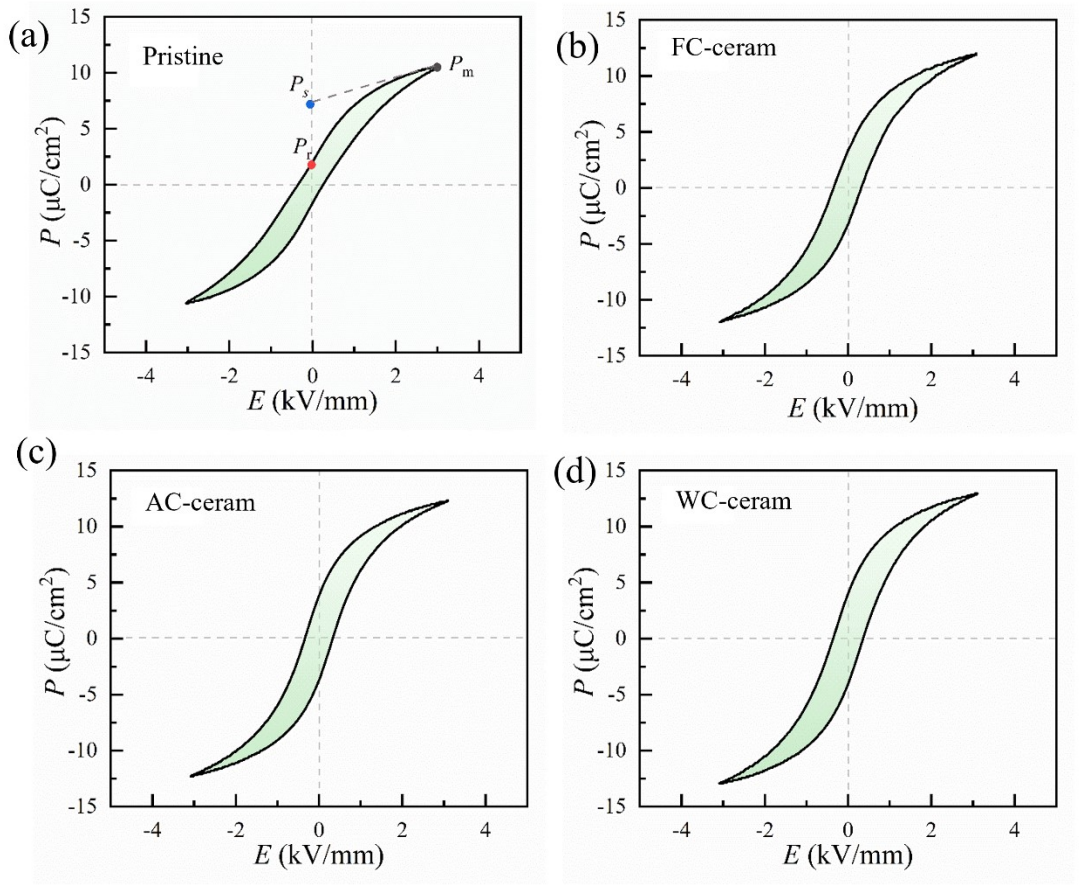

Fig. S12 Ferroelectric hysteresis (*P*-*E*) loops of (a) the pristine one, (b) FC-ceram, (c) AC-ceram and (d) WC-ceram.

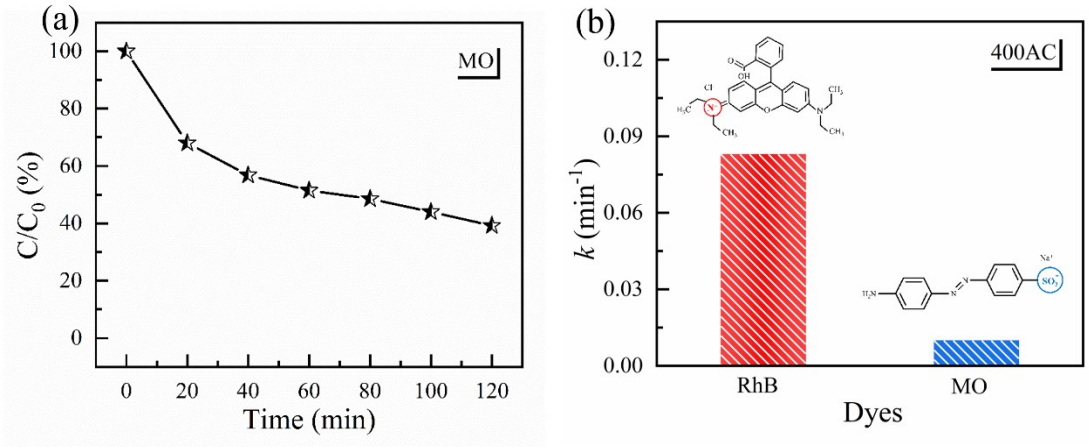

Fig. S13 (a) Time-dependent C/C_0 of MO degradation on 400AC. (b) Comparison of the *k* value of MO and RhB degradation on 400AC.